*Available online at*www.scholarsresearchlibrary.com

Scholars Research Library

Archives of Applied Science Research, 2015, 7 (4):7-22
(http://scholarsresearchlibrary.com/archive.html)

ISSN 0975-508X
CODEN (USA) AASRC9

Quantitative characterisation of groundroll (Rayleigh Waves) in the Western Niger Delta, Nigeria

Aniwetalu Emmanuel U. and Anakwuba Emmanuel K.

Department of Geological Sciences, Nnamdi Azikwe University, Awka, Nigeria

---

ABSTRACT

A study of the character and dispersion patterns of groundroll was undertaken in Western Niger Delta in order to provide much needed information and solution for its suppression during seismic surveys. The quantitative analysis was carried out on raw monitor seismic records. The results revealed the occurrence of groundroll with predominant phase velocities of 500-1020 ms^{-1} (mean of 780 ms^{-1}), frequency content of 4.0-9.0Hz (mean of 6.1Hz), wavelength of 61-240m (mean of 122m) and group mean velocity of 787 ms^{-1}, with average standard deviation of 158 ms^{-1}. The uphole data acquired was analyzed through direct or analytical determination of weathering velocities and thicknesses. The results shows that weathering and sub weathering velocities vary between 510 - 1012ms^{-1} with average value of 770ms^{-1} and 1368- 2474ms^{-1} with an average value of 1734ms^{-1} respectively. The determined thicknesses of the weathering layer ranges from 3.8 to 52.8m with an average value of 19.4m. The result showed that the weathering and sub weathering velocities as well as thicknesses of the weathering layers in the study area vary erratically both vertically and laterally. The result further showed that western Niger Delta is not a homogeneous half space but exhibits non homogeneous character with unequal phase and group velocities as well as variations in the thicknesses of the layers. This behavior showed that western Niger Delta is dispersive in nature which occurs as a result of velocity layering. The attenuation strategy designed has shown that elaborate geophone array of 28m and source pattern of 122.5m can provide excellent suppression of the bands of the wavelengths of noise in this area of study.

Keywords: Rayleigh wave, dispersion pattern, uphole data, low velocity layer and Niger delta.

INTRODUCTION

The objective of petroleum exploration is to locate pay zones – commercially viable reservoirs. The reliability of seismic mapping for determination of these zones is strongly dependent upon the quality of the seismic records. Any event that is added to the seismic signals in the course of generating, recording and processing of the seismic data is regarded as groundroll (seismic noise), and this has been the major problem to the exploration geophysicists because it often interferes with the reflection of interest.

Groundroll (Rayleigh waves) have their most natural classifications in terms of dispersion patterns. Dispersion pattern is the relationship between phase velocity, frequency and wave number [15]. Raleigh waves can be dispersive or non dispersive. Dispersive Rayleigh waves result from the various frequency components propagating at different velocities. Conversely, non dispersive Rayleigh waves result from different frequency components propagating at the same velocity. All seismic waves exhibit dispersive behavior in a medium which displays

attenuation [6] and [9]. [5] discussed the properties of Raleigh waves and showed the relevance of these noise properties in Delaware Basin. He concluded that the observed wave speed and amplitude of ground roll can be related to the velocities of the layer near the surface. [14] analyzed the dispersion properties of the first three relay modes for the case of a simple layer overlying a half space. They demonstrated the dependence of the dispersion curves on the layer thickness and contrast between the body wave velocities and densities of the two media. [12] investigated the statistical properties of Rayleigh waves due to scattering by topography, and they showed that horizontal dimension of surface morphology affect the amplitude spectra of scattered Rayleigh waves resulting from P-wave conversion and direct Raleigh wave reflection. They also argued that the scattered Rayleigh waves arriving from broadside azimuth in a true sequential display would resemble true long- wavelength P-waves. They concluded that such noise would suffer weak attenuation in data processing, thus suggested the use of source and receiver array with omnidirectional attenuation characteristics for its suppression. [18] discussed the signal characteristics and instrument specifications and gave arrangement of arrays and spreads for handling groundroll problems. Their study shows that attenuation of groundroll is possible by proper specification of array and spread geometry. [25] observed that the variation of thickness and velocity of the weathered layer within the layer could both be horizontal and vertical and more also, rapid and erratic. These weathering layers are generally related to material above the water table or geologically recent unconsolidated sediments on the substratum of harder consolidated rocks. These weathered layers (LVL) by geophysicists appear to have little to do with geologic weathered layer which denotes the disintegration of rocks under the action of denudations [13]**.** Despite the variation in the thicknesses and velocity of the LVL, the layer also varies in lithology, density and attenuation effects [21]. These variations in the physical properties of the low velocity layers (LVL) can cause a drastic deterioration in the quality of land seismic data if we do not acknowledge them and take appropriate action during data acquisition. Because the main problem in seismic reflection work is the detection of the primary P-wave signal against a background disturbing events such as ambient noise, surface waves, and secondary P and S waves produced by conversion. In particular, coherent linear noise in form of groundroll, guide waves and side scattered energy commonly obscure the genuine seismic reflections that can give useful information about the subsurface geologic features.

An important deduction from all these, is that there is ever increasing need to tailor seismic acquisition programme to the specific environment of exploration project because of environmental geologic layers differences. This is because low velocity layer (LVL) acts as a variable low pass filter or a high-cut filter on the amplitude spectrum and also cause distortion of the wavelet. Therefore, prior knowledge of these effects helps geophysicists to plan seismic acquisition techniques that can considerably reduce seismic noise**.**

However, in this study, we concentrate on the quantitative determination of the nature and dispersion characteristics of groundroll (Rayleigh waves), weathering and subweathering velocities and thicknesses of these layers using seismic reflection and uphole data (which provide useful information on weathering velocities and thicknesses of the layers as it affect the seismic travel times) in the Western Niger delta, so as to determine the general behavior of the groundroll, with view of designing the proper specification of array and spread geometry in the field.

Location and Geology of Niger delta

The study area covers towns like Orugbene, Burutu and Odimodi in the Western Niger Delta, Nigeria (Figure 1.0). It is situated on the continental margin of Gulf of Guinea in equatorial West Africa, at the southern end of Nigeria bordering the Atlantic Ocean between latitudes 3^o and 6^o and longitudes 5^o and 8^o. Known oil and gas resources of Niger Delta rank the province as the twelfth largest in the world, with 2.2% of the world's discovered oil and 1.4% of the world discovered gas (annual statistical bulletin). The Niger delta is one of the most prominent basin in West Africa and actually the largest delta in Africa [21]. The Niger Delta Province contains only one of the identified petroleum system referred to as the Tertiary Niger delta (Akata- Agbada) petroleum system [16], [7], [18], [23], and [4]. The Niger Delta displays a concentric arrangement of terrestrial and transitional depositional environment [20]. Fluvial process control sedimentation in the lower floodplain of the delta top environment, while from the mangrove swamp coastward, tidal influence prevails. The dominant process which construct the Beach ridge and barrier complexes along the delta coast are the combination of large swell waves which approach from the Southwest and strong long shore drift which the wave generated. In the offshore, the warm guinea current prevails, operating as independent cells, under the influence of the convex seaward coastline of the Niger delta and the predominant NE-directed trend wind [20]. The above depositional process from fluvial, costal, marine, including turbidity current coupled with the rise and fall of the sea level have determined the stratigraphic fill of Niger Delta. Three main lithostratigraphic subdivisions have been recognized in the subsurface of the Niger delta complex, [22]. The basal

unit is the Akata Formation, overlain by the Agbada Formation with the topmost unit as the Benin Formation. The onshore portion of Niger delta is delineated by the geology of the southern Nigeria and south-western Cameroun as shown in Fig.1.0. The northern boundary is the Benin flank, an east-northeast trending hinge line south of the West Africa basement massif. The north-eastern boundary is defined by the outcrops of the cretaceous on the Abakaliki high and further east south east by the Calabar Flank, a hinge line bordering the adjacent Precambrian.

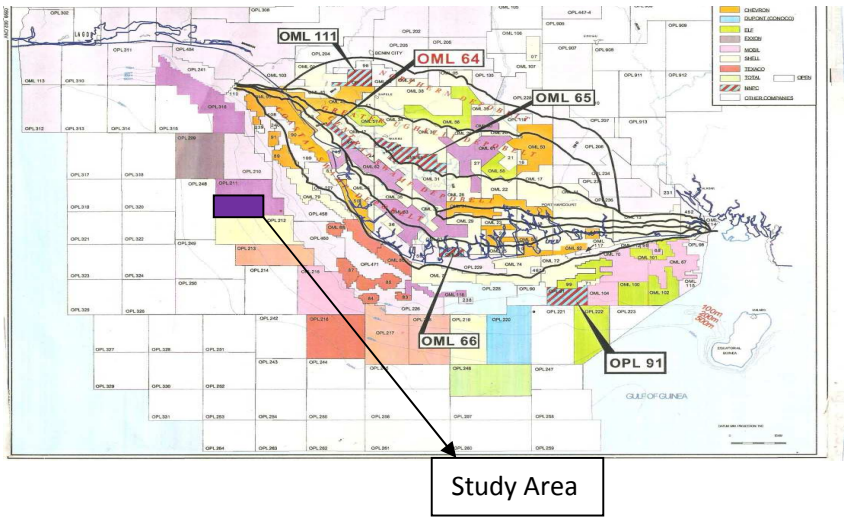

Fig.1.0: The location map of the study area

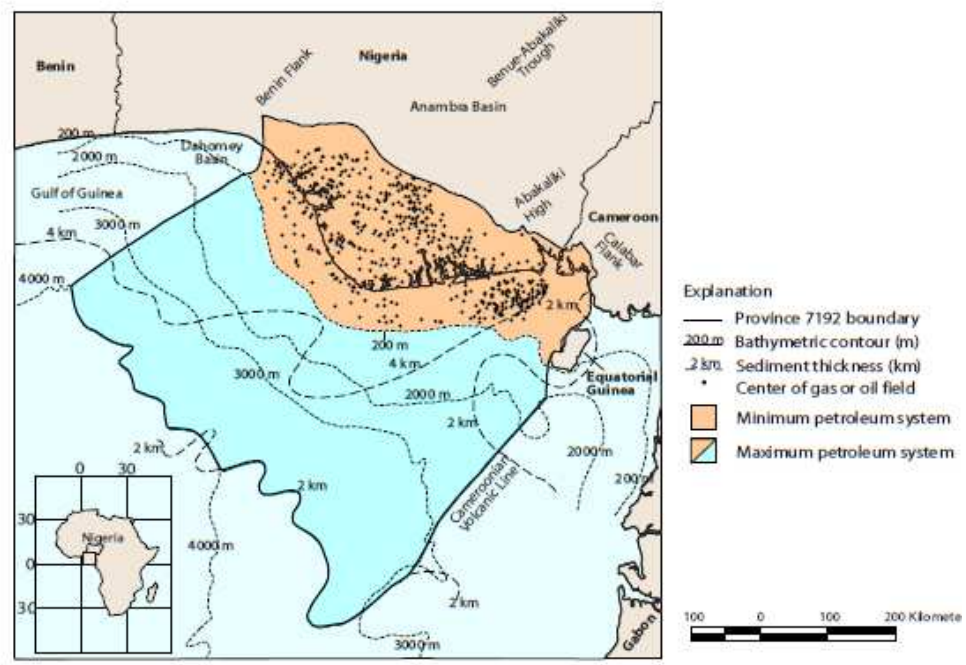

Figure 2.0: Map of the Niger Delta showing Province outline; bounding structural features; minimum petroleum system as defined by oil and gas field center points (data from Petro consultants, 1996)

MATERIALS AND METHODS

Raw seismic data acquired from seismic reflection survey, evidently marked by groundroll and uphole data acquired from seismic refraction survey in the same location were used for this analysis. The seismic lines were oriented NE – SW (Inline) and E –W (cross line) in apparent conformity with the structural trend in the Niger Delta. Values Like 1437, 1466, and 450847,450848, were assigned to the shot-points and receiver line respectively for easy referencing. Because the area of study is partly swampy, the detectors were geophones and hydrophones. Swath shooting technique was adopted. Swath or block consists of some mutually perpendicular lines (receiver and shot lines) laid out on the ground as shown in Fig. 3.0. The receiver lines consisted of 120 groups of detectors. Eighteen geophones were planted per group. Interval of 50m and 2.28m were used per group and adjacent geophones respectively. Seismic reflection record obtained during this exercise was evidently marked by groundroll (seismic noise) as shown in Fig. 4.0

In acquiring the uphole data, each shot hole was initially planned to be drilled to a depth of 72m with the aim of recovering a minimum depth of 60m. With 60m control depth, an interval of 5m was chosen for each charge detonation. Charges were successfully detonated, starting from the bottom and the travel time recorded using geophone planted on top of the earth surface near the shot hole.

However**,** a quantitative method was used to analyze the character and the dispersion pattern of groundroll from raw monitor records. In this approach, seismic attributes of groundroll such as phase and group velocities, periods, wavelengths, wave number and frequencies were measured or computed manually from the raw record. This method gives good parameter estimate, although it is time consuming and results of such computations may be error bound because of the numerical approximations inherent in the analysis. Nevertheless, extra care was taken to achieve quality results.

Phase velocity is the speed at which a point of constant phase can be said to move or the rate at which the fixed phase of the wave propagates in space. Thus,

$x/\lambda - ft=k$ 1

Where x, λ, t, f and K stand for distance, wavelength, frequency and constant respectively.

So the phase velocity V_P is given by

$$\frac{dx}{dt} = \lambda f \quad [16] \qquad 2$$

In the computation of phase velocities from the raw monitor record, consider the onset of noise in Fig. 4.0 as indicated by Triangle ABC. The triangles ABC consist of two right angled triangles ACD and ABD. The slopes AB and AC are symmetrical. The distance BD equals CD (68 trace spaces), where one trace space corresponds to 50m. The first arrival time is 5seconds. Therefore the phase velocity of the groundroll (using the slope of the line) was calculated from the distance/ time relationship.

In some cases, several waves add together to form a single wave shape known as envelope or group velocity. Group velocity describes the rate at which the envelope of wave travels through the dispersive medium. It is defined by

$U = \frac{w}{k}$, 3

Where U, w and k stand for group velocity, angular frequency and wave number respectively.

The group and phase velocity are related by the equation

$$V = U[\,1 - \frac{f}{V} * \frac{dv}{df}] \quad [16] \qquad 4$$

Where V, U,and f, stand for phase velocity, group velocity and frequency.

The equation shows that if phase velocity (V) is independent of frequency, then U=V, but if V decreases with increasing F, which occurs if shear wave velocity increases with depth, then,

$$\frac{dV}{dF} \leq 0 \qquad 5$$

and phase velocity will exceed or equal the group velocity as in the case of **normal dispersion**. However, in **anomalous dispersion**, phase velocity increases with increasing frequency. Thus, the group velocity exceeds or equals phase velocity as demonstrated in Table1.0,Group velocities were computed from fig.4.0 using equation 3.0.
Period is the duration of one cycle in a repeating event. The period (T) was determined from the raw monitor record as an interval time from peak to peak or trough to trough. The raw monitor record data has a scale of 5cm to 1sec. Based on this, the distance between two crests or troughs were measured and compared with the scale. In fig. 4.0 for instance, the distance between two peaks designated as M^1 and M is 1cm. Since 5cm represents one second, then 1cm is equivalent to 0.20sec which is the period.

Frequency is the number of occurrence of a repeating event or oscillation per unit time. It is the reciprocal of period, measured in Hertz. It was calculated using the relation

F= 1/T. [16] 6

Where F and T stand for frequency and Period.

Assuming a sinusoidal wave moving at a fixed wave speed, wavelength is inversely proportional to the frequency and directly proportional to the velocity of the wave.

$$\lambda = \frac{V}{F} \qquad 7$$

Where V, F and λ are phase velocity, frequency and wavelength respectively.

Already, the phase velocity, and frequency have been determined. Wavelength was determined using equation 7.

Wavenumber (k) is the property of a wave, proportional to the reciprocal of the wavelength. It can be defined as the number of wavelength per unit distance that is

$$k = \frac{1}{\lambda} \qquad 8$$

Where k and λ stand for wavenumber and wavelength

The results of all these wave characters were individually calculated with respect to their event numbers and presented in Table 1.0

The analysis of the Uphole data is simple and direct, and with little calculations. The basic methods for the analyses are as follows [25]

(i) The arrival time at each depth was picked and recorded.
(ii)The picked travel times were plotted against their corresponding depth of shot known as time depth plot.
(iii) The weathering velocities (V_w) and sub weathering velocities (V_{sw}) were computed from the inverse of the corresponding graph slopes.
(iv) The weathering thickness, D_w is graphically or analytically obtained.

Alternatively, the weathering layer thickness, D_w can be determined analytically. If we consider fig. 5.0, we have from the two graphs segments that

$\mathbf{Y = b_1x}$ (graph from origin) 9
$\mathbf{Y = b_2x + a}$ (graph not from origin) 10
For the two straight lines, at crossover point, equations 9 and 10 are equal, that is

$$b_1x = b_2x + a \quad (11)$$

So

$$x = \frac{a}{b1-b2} \quad (12)$$

By substituting equation 12 into 10 or 11, gives the thickness of the weathered layer. Thus

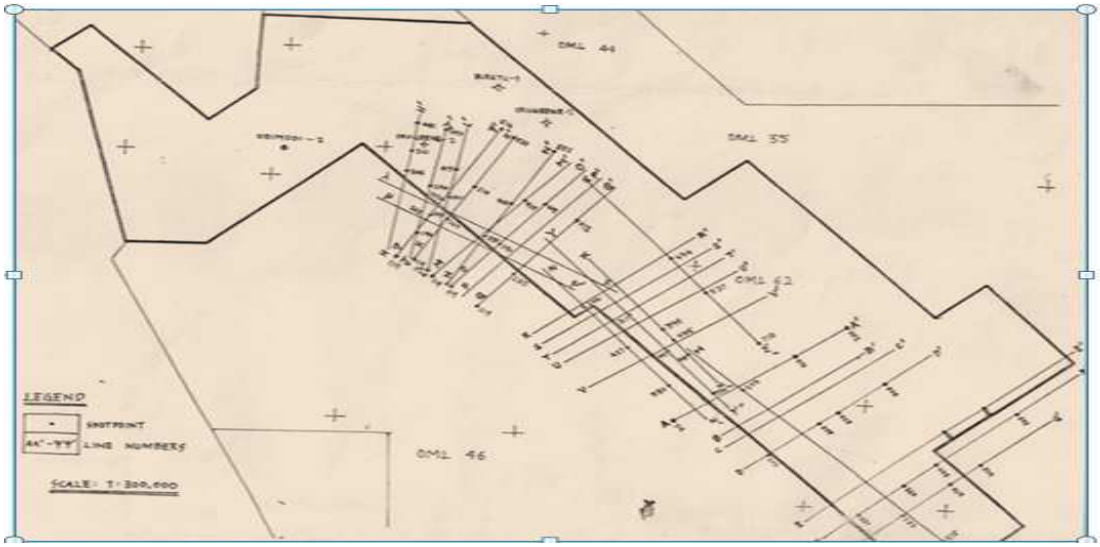

Fig.3.0: The Swath method of acquisition

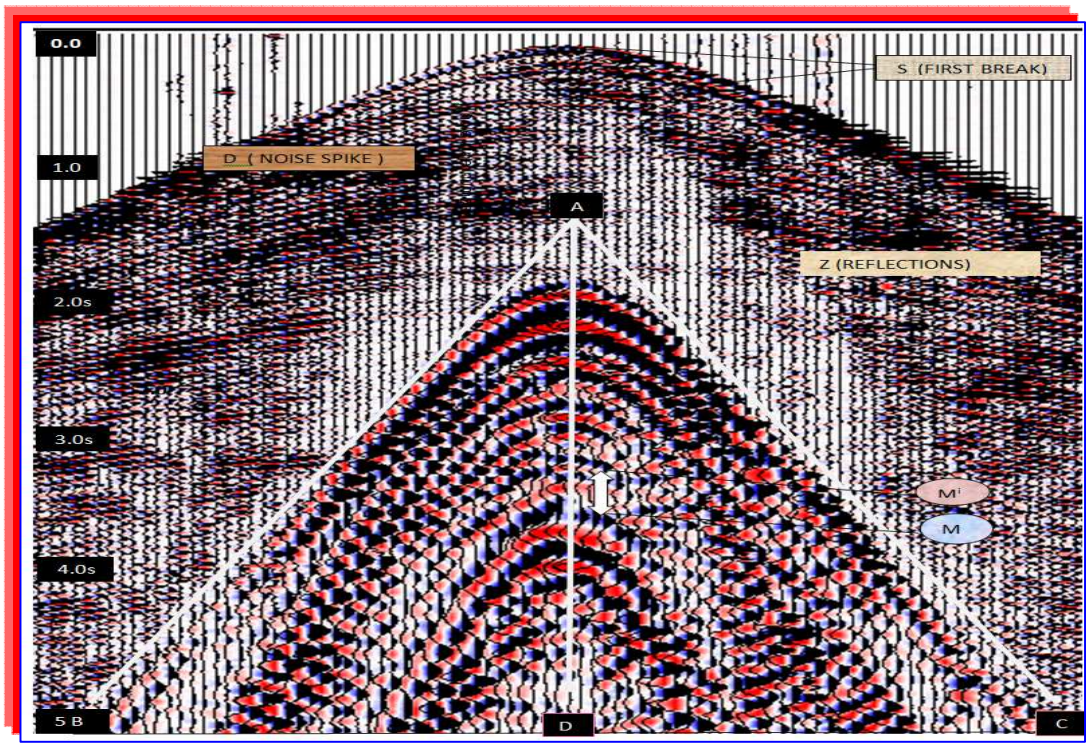

Fig.4.0: Raw seismic reflection data showing Rayleigh waves (seismic noise) as indicated in triangle ABC

$$D_w = \frac{b1\ a}{b1-b2} = \frac{b2a\ +a}{b1-b2} \qquad 13$$

Where b_1 = slope of first graph (in milliseconds per meter)
b_2 =slope of the second graph (in milliseconds per meter)
a = intercept time, T_i of the second segment (milliseconds)
D_w = thickness of the weathered layers
y and x stand for graph axes

The reciprocal of b_1 and b_2 give the weathering layer and the sub weathering layer velocity respectively. Direct substitution of the values of a, T_i, b_1 and b_2 into equation 5, gives the thickness of the weathered layer. This method is mathematically and accurately competent.

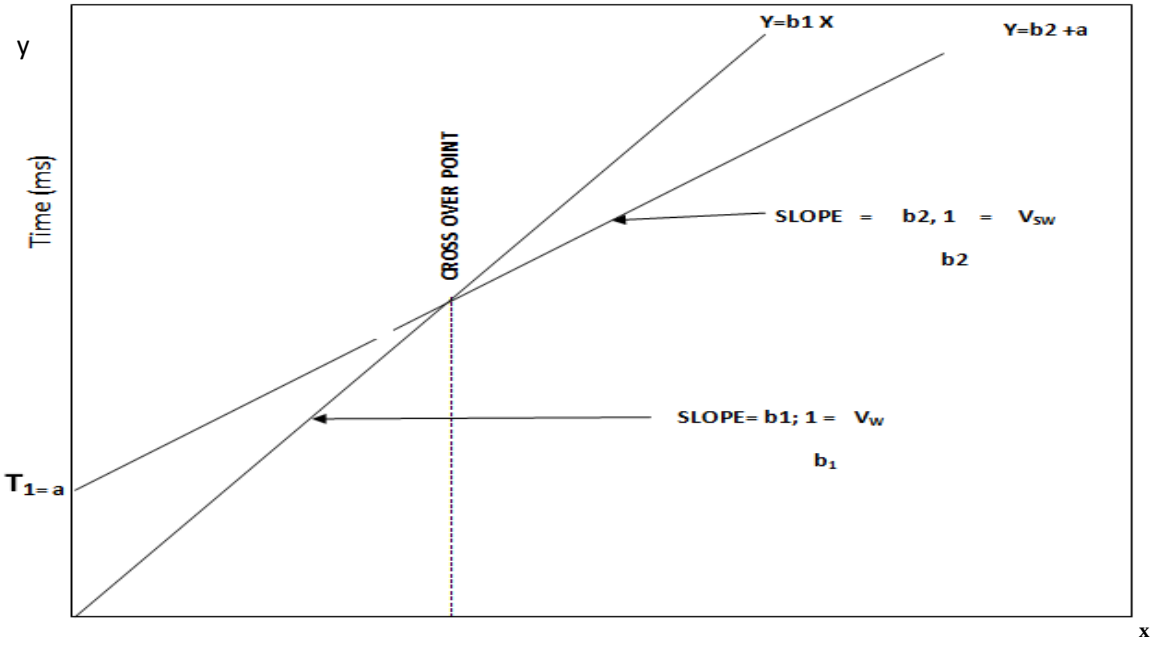

Fig.5.0: Techniques for weathering, sub-weathering velocity and thickness determination fromt uphole data

RESULTS

The calculated seismic parameters (Trace values, Phase and Group velocities, Period, Frequency, Wavelengths, and wave number) of groundroll are displayed in Table 1.0. They represent the seismic attributes of the event in each data location.

Phase and Group velocities

The results from the raw monitor record show that groundroll (seismic noise) has phase velocities in the range of 500-1020ms^{-1}, mean of 780ms^{-1}, standard deviation of 154 and mode of 740ms^{-1} (Table 2.0). The histogram plot of the computed phase velocities shows that the maximum value peaks between 700ms^{-1} and 800ms^{-1}, indicating the predominance of groundroll in this region (Fig. 6.0).The group velocity values range from 510-1040ms^{-1}, a mean velocity of 787ms^{-1}, a standard deviation of 158ms^{-1} and mode of 714ms^{-1}(Table 2.0,).

Table 1.0: Some computed groundroll parameters of the study area

Event no	Number Within Line	Shot point no	Trace values (m)	Trace interval (m)	Phase velocity (ms-1)	Group velocity (ms-1)	Period (s)	Frequency (Hz)	Wavelength (m)	Wave numbers
1	450847	1437	68.00	50	680.00	685.00	0.20	5.00	163.00	0.0073
2	450848	1466	77.00	50	770.00	772.00	0.16	6.25	123.20	0.0081
3	450849	1496	73.00	50	730.00	736.00	0.14	7.14	102.24.	0.0097
4	450850	1528	64.00	50	640.00	641.00	0.12	8.33	76.83	0.013
5	450851	1560	50.00	50	500.00	510.00	0.16	6.25	80.00	0.0125
6	450852	1593	96.00	50	960.00	965.00	0.14	7.14	134.50	0.0074
7	450853	1627	91.00	50	910.00	920.00	0.16	6.25	145.60	0.0069
8	450854	1662	70.00	50	700.00	714.00	0.11	9.00	70.00	0.014
9	450855	1698	68.00	50	680.00	694.00	0.12	8.33	81.63	0.012
10	450856	1735	62.00	50	620.00	625.00	0.16	6.25	99.20	0.010
11	450857	1772	82.00	50	820.00	820.00	0.12	8.33	98.43	0.010
12	450858	1809	85.00	50	850.00	856.00	0.16	6.25	136.00	0.0073
13	450859	1848	95.00	50	950.00	957.00	0.12	8.33	114.00	0.0087
14	450860	1886	101.00	50	1010.00	1011.00	0.18	5.55	181.80	0.0055
15	450861	1926	102.00	50	1015.00	1025.00	0.16	6.25	163.20	0.0061
16	450862	1966	82.00	50	820.00	822.00	0.16	6.26	131.00	0.0076
17	450863	2006	99.00	50	990.00	991.00	0.18	5.55	179.00	0.0056
18	450864	2047	113.00	50	1015.00	1025.00	0.16	6.25	180.80	0.0055
19	450865	2088	86.00	50	860.00	856.00	0.22	4.54	189.00	0.0053
20	450866	2130	74.00	50	740.00	746.00	0.20	5.00	148.00	0.0067
21	450867	2172	88.00	50	880.00	881.00	0.14	7.14	123.25	0.0081
22	450868	2214	98.00	50	980.00	980.00	0.22	4.50	220.00	0.0045
23	450869	2254	64.00	50	640.00	641.00	0.12	8.33	73.83	0.0130
24	450870	2297	65.00	50	650.00	667.00	0.11	9.00	65.00	0.015
25	450871	2340	58.00	50	580.00	584.21	0.18	5.55	104.50	0.0095

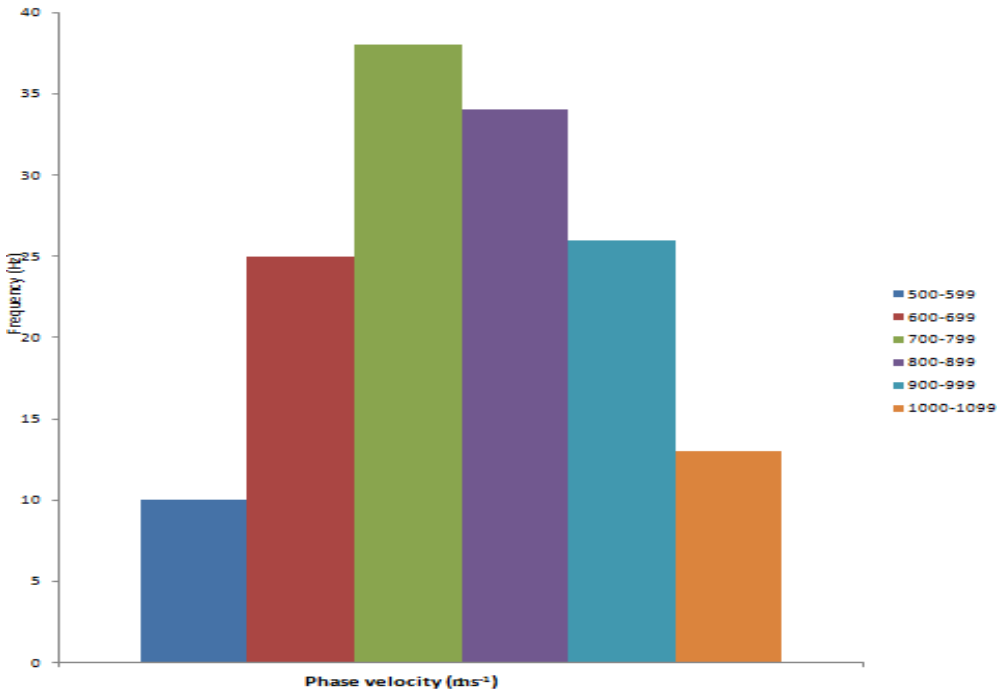

Fig. 6.0 Histogram plots of velocity distributions of the study area

Table 2.0: The statistical values of the groundroll parameters of the study area

PARAMETERS	MEAN	MODE	MEDIA	VARIANCE	STANDARD DEVIATION
PHASE VELOCITY	780	740	785	23648	154
GROUP VELOCITY	787	714	782	24897	158
FREQUENCY	6.10	8.33	7.14	2.4855	1.60
PERIOD	0.15	0.12	0.14	0.0015	0.039
WAVE LENGHT	122	130	110	1827.80	43

The result of the data analyzed had shown variations in the periods of seismic wave in the raw monitor records (Table1.0). The periods of the study area have mean value of 0.15s, mode of 0.12s and the standard deviation of 0.039s. These low values of periods in the area could be attributed to the low oscillation of wave front which depends on the frequency and phase velocity of the wave train. The result also shows frequency content of 4.16-9.0Hz, which produced the mean value of 6.10Hz, mode of 8.33Hz and standard deviation of 1.6Hz. The wavelength distributions vary between 61-240m with mean value of 122m, standard deviation of 43m and mode of 130m. The bar chart plot in Fig.7.0 shows wavelength peak at 101m and 120m, suggesting the predominance of the

wavelength of groundroll energy in the study area. This perhaps, is the fundamental propagating wavelengths of the groundroll in the study area increasing to 240m for the longest wavelength.

[1] and [23] have shown the dependence of Rayleigh wave, phase and group velocities on frequency for propagation in a homogeneous half space and in layered medium. He showed that phase and group velocity values are equal and independent of frequency, which results in non dispersive behavior. This is undoubtedly is in contrast with the computed group and phase velocities in the study area as shown in fig.8.0 and 9.0. In non dispersive Rayleigh waves as he stated, all frequency components propagate at the same velocity. The result for an impulsive source, such as an explosion in this environment is that the Rayleigh wave has a sharp onset, a short duration and a uniform wavelet shape at all offsets. In other words, the output wavelength is identical to the input wavelength with time delay. This character only described the non dispersive environment. In dispersive environment which our results exhibit, different frequency components travel at different velocities as a result, the phase velocity which is the rate at which the fixed phase of the wave propagates is unequal with the velocity of the envelope known as the group velocity as shown in figure 8.0. In fig. 9.0 , the phase and group velocities were plotted as a function of frequency on a semi-log graph. A close look at this plot shows that curves are concave. There is a uniform decrease of the curves to the lowest limit of velocity values before they rise again. These lowest points of velocities are probably the limit of the overhead layer also known as low velocity layer (LVL). However, the phase velocities plot is lower than group velocities which are an indication of dispersive environment. It is important to note therefore that this dispersion curves are different from those plotted by [11]. [11] corresponds to uniform single layers (Homogeneous media), instead in this study corresponds to non homogeneous layered media

Three Rayleigh modes which have been designated as fundamental, first higher Rayleigh mode and second higher Rayleigh mode are evident in the study area (Fig.10.0). The first and second Rayleigh modes plot higher whiles the fundamental Rayleigh mode plot lower. This demonstrates the pattern of distribution of the phase velocity of Rayleigh mode in the western Niger delta. However, the first and second higher Rayleigh modes result from the constructive interference between shear waves trapped between the interfaces of the shallow layers. This is in contrast to fundamental Raleigh mode which results from diffraction of the spherical wave fronts of the body waves at the interface between the earth and the atmosphere. In the higher modes, the decay of the amplitude with depth resemble standing waves in organ pipe as depicted in Fig.11.0. This illustrates the qualitative variation of amplitude with depth for three Rayleigh modes in two layered model

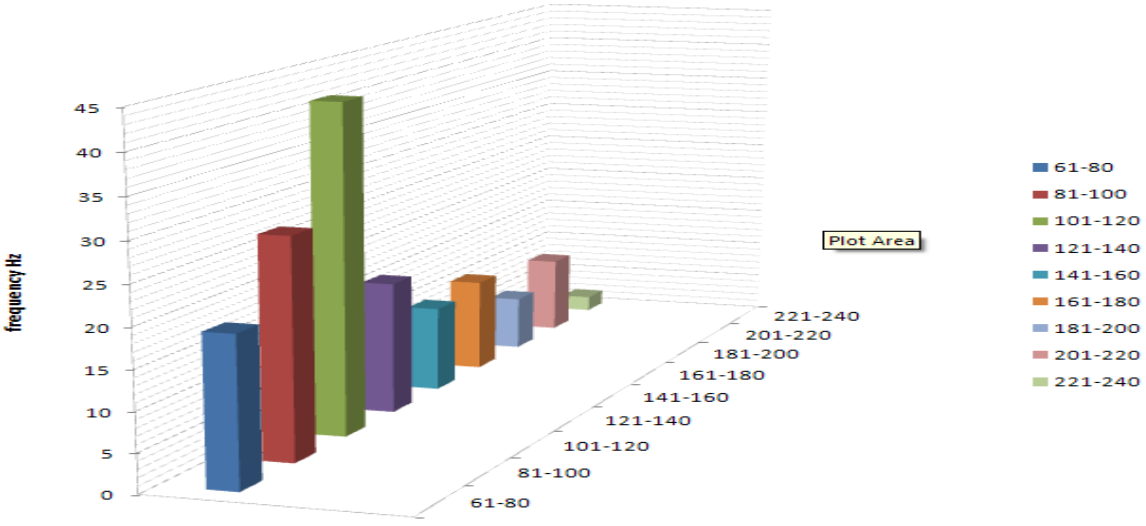

Fig. 7.0 Barchart showing wavelength distributions in the study area

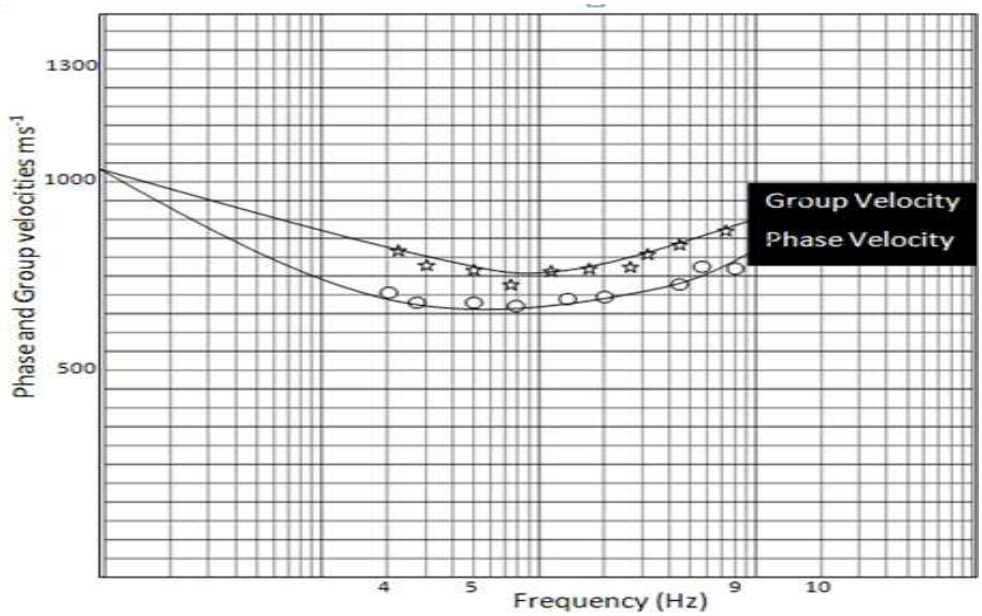

Fig.8.0: The dispersion curve of the study area

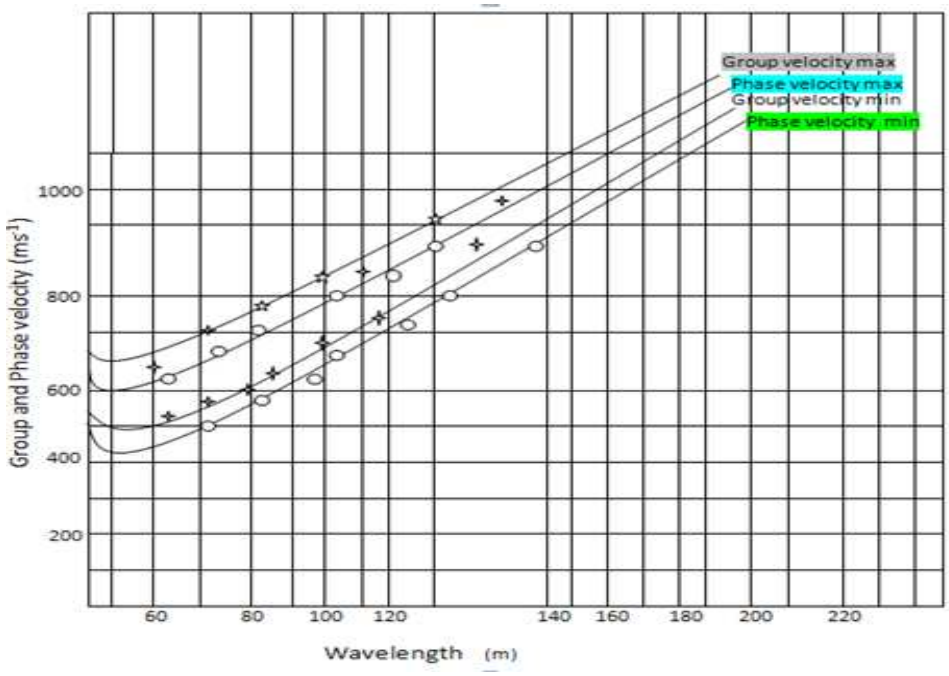

Fig. 9.0: Plot of phase and group velocities against wavelength showing dispersion pattern of the waves in the study area

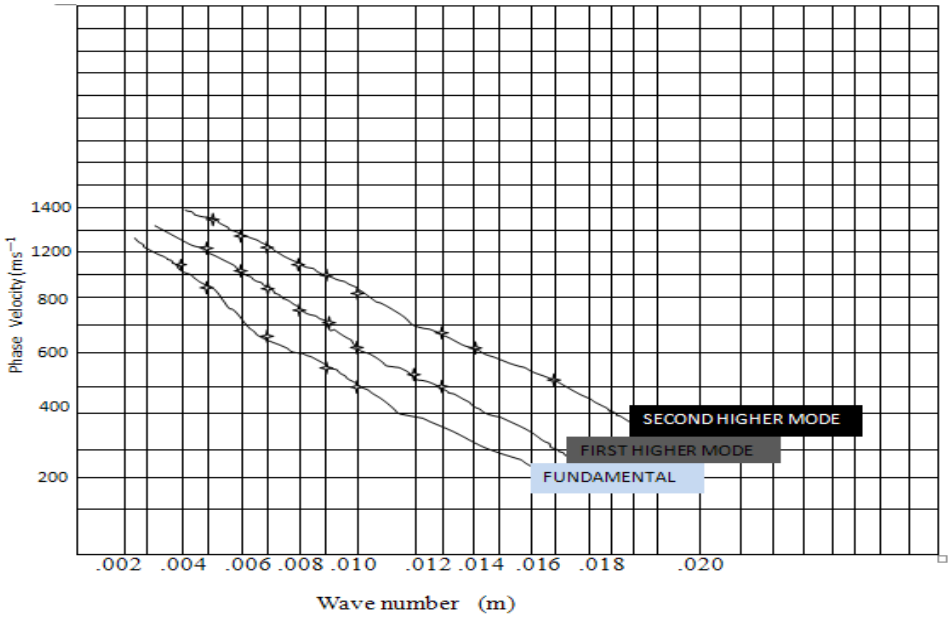

Fig. 10.0 : The pattern of distribution of the phase velocity of Rayleigh mode in the western Niger delta

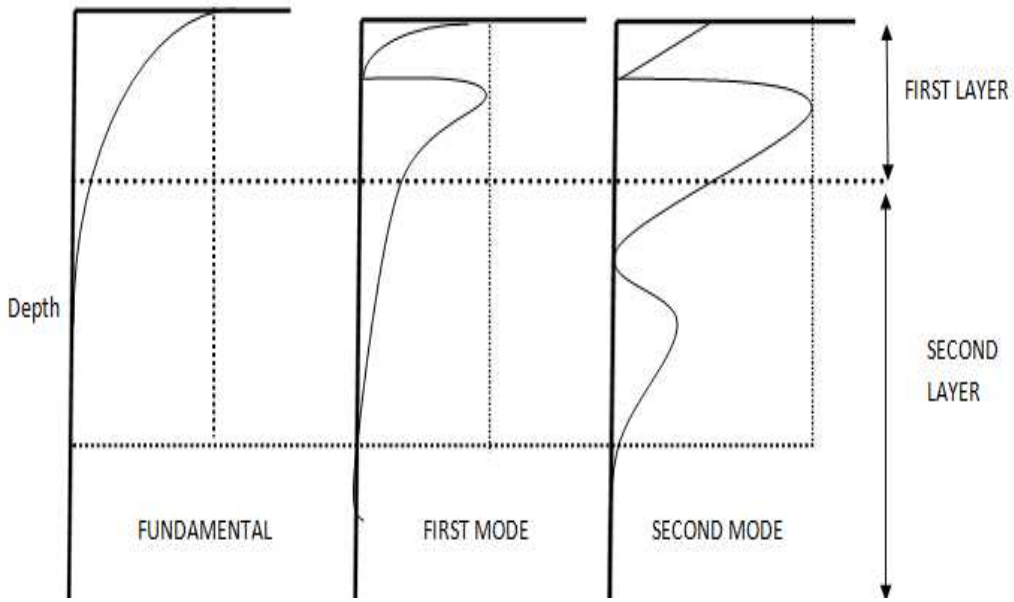

Fig.11.0: Qualitative variation of amplitude with depth for three Rayleigh modes

In Fig 12a-d and Table 3.0, weathering velocities, sub weathering velocities and thicknesses of the weathering layer vary erratically both vertically and laterally in the study area. Weathering velocities of 510 to 1012ms^{-1} with an average value of 770ms^{-1} from the Time-depth plots were determined while the sub weathering velocities vary from 1368 to 2474ms^{-1} with an average value of 1734ms^{-1}.

The thicknesses of the weathering layer ranges from 3.8 to 52.8m with an average value of 19.4m. The values of the velocity and thickness profile from Uphole plots in Fig.12a-d indicate that two velocity layers could be identified with varying thicknesses in the study area.

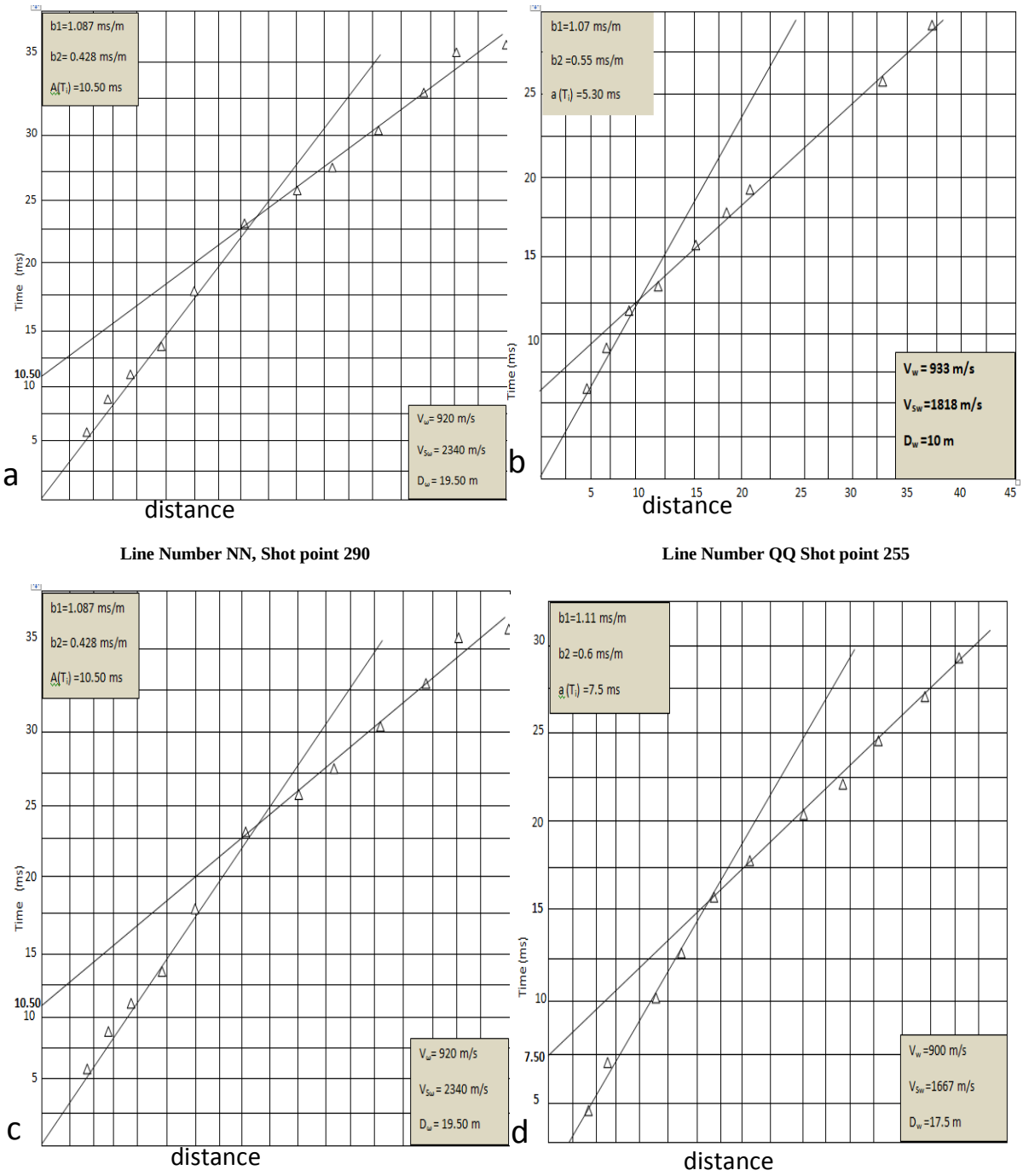

Line Number NN, Shot point 290 **Line Number QQ Shot point 255**

Line Number ΦΦ; Shot point 225 **Line Number KK; Shot point 119**

Fig.12a-d: Time-Distance graphs of some selected line number KK; Shot point 119

Table 3.0: Results of LVL parameters of the study area

S/NO	LINE NO	SHOTPOINT	V_W(m/s)	V_{SW}(m/s)	D_W (m)
1	AA”	199	994	1647	10.9
2	“	470	857	1863	12.1
3	“	552	700	1610	6.3
4	DD”	203	950	1670	24
5	“	358	785	2300	19.0
6	“	425	910	1997	12.8
7	“	508	890	2000	14.0
8	EE”	554	800	1590	3.8
9	“	664	710	1500	5.5
10	FF	221	925	2090	12.0
11	“	360	800	1600	3.5
12	“	448	820	1820	5.3
13	“	690	1000	1700	5.6
14	GG”	282	573	1640	8.4
15	“	429	734	1821	3.7
16	“	509	586	1450	10.0
17	HH”	306	505	1976	18.5
18	“	361	676	1552	30.0
19	“	441	529	1455	23.8
20	II”	303	900	2119	33.4
21	“	975	850	1981	25.8
22	“	116	950	1952	28.5
23	JJ”	196	658	1739	14.7
24	“	294	750	1686	44.2
25	“	490	887	1652	10.6
26	KK”	119	900	1667	17.5
27	“	246	645	1802	21.8
28	“	374	710	1657	10.9
29	“	520	590	1723	27.0
30	LL”	119	530	1449	18.9
31	“	284	781	1641	22.2
32	“	341	724	1746	14.3
33	“	417	562	1813	32.0
34	MM”	199	694	2475	52.8
35	“	429	512	1826	25.5
36	NN”	119	709	1358	33.5
37	“	290	920	2340	19.5
38	“	400	600	1711	25.2
39	“	552	736	1730	25.9
40	OO”	119	882	1984	35.5
41	“	290	870	1852	14.0
42	“	442	823	1666	25.9
43	QQ”	225	933	1818	10
44	“	227	820	1641	13.5
45	“	473	545	1666	24.1
46	WW”	434	692	1873	17.4
47	“	537	670	1747	26.8
48	“	110	515	1686	18.5
49	XX”	389	756	2240	19.3
50	“	432	565	2464	28.3
51	“	469	850	1595	13.1
52	YY”	317	722	1774	15.9
53	“	447	650	1900	23.8
54	“	650	651	1836	19.1
55	ZZ”	226	600	1635	33.9
56	“	427	726	1698	11.9
57	“	580	770	1549	14.1
58	ΦΦ”	119	822	1665	19.5
59	“	265	776	1611	11.6
60	“	350	900	1667	17.5
61		516	650	1594	19.8
	AVERAGE		770 m/s	1734m/s	19.4m

Maximum weathering thickness of 52.8m was observed northward, on line number MM, shot point 199. On the other hand, a decrease in the thickness trend was observed southward, which is toward the coast, at line number EE shot point 554 in the south (Table 3.0). Uphole P-wave velocities (table 3.0) compares favorably with velocities of groundroll in table 1.0 which show that two seismic events travel through the same layer (surface layer), thus validating our results. However, because of the variation in the thicknesses of these surface layers, waves propagate at different velocities. We therefore, suggest that the dispersive character of the Rayleigh waves or groundroll in the western Niger delta occur as a result of velocity layering.

These weathering layers, affect seismic data in a variety of ways: The rapid changes in the velocity and thickness of this layer has a disproportionately large effect on the travel times

The absorption of seismic energy is high in this layer since the layer is unconsolidated. The marked velocity change at the base of LVL sharply bends seismic rays so that their travel time through the low velocity layer is nearly vertical regardless of their direction below the weathering layer.

There is very high impedance contrast at the base of the LVL, which makes the weathering layer an excellent reflector. Consequently, waves remain trapped in the layer, repeatedly reflecting from its base and its upper surface, thereby becoming an important multiple reflector that is vital in mode conversion [8]

Since suppression of groundroll starts in the field, it is imperative to design a geophone arrays and source pattern that can provide excellent attenuation of band wavelengths of the noise in the study area. From the Table 1.0, the minimum and maximum velocities are 500 and 1020m/s, while the minimum and maximum frequencies are 4.16 and 9.0Hz respectively. Thus, the array must attenuate a band of wavelengths bounded by

$$\frac{Vmax}{Fmin} \geq \lambda \geq \frac{Vmin}{Fmax} \qquad 14$$

i.e. $$\frac{1020m/s}{4.16Hz} \geq \lambda \geq \frac{500m/s}{9.0Hz}$$

$$= 245m \geq \lambda \geq 55.6m$$

Therefore, this implies that geophone or source pattern with half the wavelength (i.e. 28m and 122.5m) can creates an array arrangement that will suppress the band wavelengths of the type of groundroll in the area. The design of this pattern from array theory was based on the following assumptions, that
(i) There was uniform output from the different geophones
(ii) All geophones were similarly and precisely coupled to the ground
(iii)The topography was level.

CONCLUSION

In this research, we have illustrated the properties of dispersive Rayleigh waves chiefly by means of interpreted observations from the computed groundroll attributes integrated with uphole data. However in comparing the dispersive Rayleigh waves with non dispersive Rayleigh waves, the following differences were noted. First, on any given offset trace, the dispersive Rayleigh wave exhibit a long duration. In the case of half space, the phase and group velocities respectively are identical and independent on frequency but in non homogeneous media, phase and group velocity are not identical and thus propagate with different frequency. The phase velocity determines the apparent wavelengths and therefore has immediate relevance in the design of source and receiver arrays. This can be understood where array pattern was designed for the study area. Weathering velocities, sub weathering velocities and thicknesses of the weathering layer vary erratically both vertically and laterally in the study area. Weathering velocities of 510 to 1012ms^{-1} with an average value of 770ms^{-1} from the Time-depth plots were determined while the sub weathering velocities vary from 1368 to 2474ms^{-1} with an average value of 1734ms^{-1}. The determined thicknesses of the weathering layer ranges from 3.8 to 52.8m with an average value of 19.4m. Three Rayleigh modes have been identified in the study area, Higher Rayleigh modes result from constructive interference between shear waves trapped between the interfaces of shallow layers of this environment. This is in contrast to the

fundamental Rayleigh mode which results from the diffraction of the spherical wave-front of the body waves at the interface between the earth and the atmosphere.

Furthermore, based on the observed results in the area of study, Rayleigh waves exhibit dispersion pattern that are independent of source type because the relationship between velocity, frequency and wave-number depend on the properties of the medium which transmit these waves and not on the nature of the source. However Geophone or source pattern of 28m and 122.5m apart can provide excellent attenuation of noise in the area of study. Also burying the source (dynamite) below the weathering layer or adopting smaller charges could also suppress the noise in the field recording.

REFERENCES

[1] M.K Al Hussein, and T.E Barley, *Geophysics* **1981**, 46, 122-137.
[2] J.R Allen, *Geologic En Mijubio* **1965**, 44, 381-397.
[3] N.A, Anstey, Signal characteristics and Instrument specifications , **1970**,1, 12-20
[4] T.J, Arthur, **1993**. Textbook 362p
[5] N.B, Dobrin, McGraw Hill New York, **1951**, 5, 27-42.
[6] J.O Ebeniro, *Journal of mining and geology*, **1993**, 29, 183-193.
[7] C.M, Ekweozor, and E.M, Daukoru, **1994,** Texbook, 599-614p.
[8] I.R. Finetti, and S. Sancin, *Geophysics* **1971**. 19, 292-320.
[9] A.A Fitch,*Geopublications Associates* **1976**,3,105-108.
[10] E.A Flin, and, S. Treitel**,** *Geophysics*, **1967,** 32, 411-535
[11] F.S Grant, and G.E West, McGraw Hill, New York, **1965**, 132-140.
[12] J.A.Hudson, and L.A. Knopoff, *SSA Bull*, **1967**, 36, 1191-1201.
[13] M.A.Madsen, *Geophysics* **1993,** 30, 320-387.
[14] H.M Mooney and B.A. Bolt, *SSA Bull* **1966,** 56, 43-67.
[15] H.M Mooney and T.H. Kaasa, *Geophysics* **2005**, 47, 1345-1351
[16] , P.N Okeke and B.L.N Ndupu, **1983**.Textbook, 100p
[17] J.M., Orife, and A.A. Avbovbo, *AAPG Bulletin*, (1978). 66, 251-262.
[18] T.C Poulter, *Geophysics*, **1950**, 15, 181
[19] T.J Reijers, S.W., Petters, and C.S Nwajide, Amsterdam, Elservier Science, **1997,**151- 172.
[20] R.C Selley, McGraw Hill, New York, **1997,** 3, 30-42.
[21] R.E Sheriff, *Geophysics*, **1984**, 34, 56
[22] K.C Short and A.J. Stauble. *AAPG Bull* **1967**, 51, 761-779.
[23] D.I Silverman, *Geophysics*, **1967**, 32, 988- 1002.
[24] M.L.W. Tuttle, *Geophysical Survey;* USGS, **1999,** 103-104
[25] E.M. Uko, *NAPE Bull*. **1991**,6, 67-74.